Advances in Photonic Quantum Sensing

Stefano Pirandola,[1,2] Bhaskar Roy Bardhan,[3] Tobias Gehring,[4] Christian Weedbrook,[5] and Seth Lloyd[2,6]

[1]*Computer Science and York Centre for Quantum Technologies, University of York, York YO10 5GH, UK*
[2]*Research Laboratory of Electronics, MIT, Cambridge MA 02139, USA*
[3]*Department of Physics and Astronomy, State University of New York at Geneseo, Geneseo NY 14454, USA*
[4]*Department of Physics, Technical University of Denmark, Fysikvej, 2800 Kongens, Lyngby, Denmark*
[5]*Xanadu, 372 Richmond St W, Toronto, M5V 2L7, Canada*
[6]*Department of Mechanical Engineering, MIT, Cambridge MA 02139, USA*

Quantum sensing has become a mature and broad field. It is generally related with the idea of using quantum resources to boost the performance of a number of practical tasks, including the radar-like detection of faint objects, the readout of information from optical memories or fragile physical systems, and the optical resolution of extremely close point-like sources. Here we first focus on the basic tools behind quantum sensing, discussing the most recent and general formulations for the problems of quantum parameter estimation and hypothesis testing. With this basic background in our hands, we then review emerging applications of quantum sensing in the photonic regime both from a theoretical and experimental point of view. Besides the state-of-the-art, we also discuss open problems and potential next steps.

Quantum technologies are today developing at unprecedented pace. As a matter of fact, the technological applications of the field of quantum information[1–5] are many and promising. One of the most advanced areas is certainly quantum sensing. This is a broad term which encompasses all those quantum protocols of estimation and discrimination of physical parameters which are able to exceed the performance of any classical strategy. Quantum sensing improves a number of tasks, including gravitational wave detection, astronomical observations, microscopes, target detection, data readout, atomic clocks, biological probing and so on.

As with most technologies, quantum physics offers improvements that in some cases far exceed anything that can be done classically. The quantum version of sensing is no exception. By exploiting fundamental laws of physics one can leverage important quantum characteristics such as entanglement, single photons and squeezed states[5–7] in order to achieve orders-of-magnitude improvements in precision. In this scenario, the photonic regime is certainly the best setting thanks to the relative simplicity in the generation, manipulation and detection of such exotic quantum features.

This review aims to provide a survey of recent advances in photonic quantum sensing. We refer the reader to Degen et al.[8] for an overview of quantum sensing in non-photonic areas, related to spin qubits, trapped ions, and flux qubits. Here we start by providing mathematical background in quantum parameter estimation[9–15] and quantum hypothesis testing[16–25], presenting the most general formulation of these problems. In fact, we describe the most powerful (adaptive) protocols allowed by quantum mechanics and how they can be reduced to simpler schemes by employing methods of channel simulation[26,27]. This is an approach based on tools of quantum programmability[28–31] and teleportation stretching[33,34]. This general background will allow us to identify the goals, the structure, and the classical benchmarks for the following protocols of quantum sensing that we will discuss both theoretically and experimentally.

Quantum hypothesis testing is at the very basis of quantum reading[35–49], where the information stored in an optical memory (or an equivalent physical system) is retrieved by using extremely low energetic quantum states of light. It is also at the basis of quantum illumination[50–67], where the radar-like detection of remote and very faint targets is boosted by the use of quantum correlations. Quantum parameter estimation is the core idea for the most recent advances in quantum imaging and optical resolution[69–83], where "Rayleigh's curse" may be dispelled by using quantum metrological detection schemes[69–71] whose accuracy and sensitivity do not depend on the separation of two point-like sources.

Estimation and discrimination protocols

Quantum sensing takes its roots in two problems which are central in quantum information theory, known as quantum parameter estimation (or quantum metrology) and quantum hypothesis testing (or quantum discrimination). A modern formulation of these problems is respectively in terms of quantum channel estimation and quantum channel discrimination, where the task is to estimate or discriminate the values of a classical parameter encoded in a quantum channel, i.e., a transformation between quantum states. Mathematically, both the problems can be described by using an input-output formalism where two parties, say Alice and Bob, probe a black box containing the unknown quantum channel.

Therefore, consider a parameter θ encoded in a quantum channel $\mathcal{E}_\theta$ and stored in a black box, of which Alice may prepare the input and Bob may detect the output. In the estimation problem, θ is a continuous parameter, while in the discrimination problem, θ may only take a discrete and finite number of values with some prior probabilities. For the latter case, we consider here the most basic scenario: binary symmetric discrimination, where θ may only take two values, θ_0 (null hypothesis) or θ_1 (alternative hypothesis), with the same Bayesian cost and prior probability. This is then equivalent to retrieving

the classical bit u which is encoded in the parameter θ_u.

Let us analyze the estimation/discrimination problem with an increasing level of complexity. In a basic "block unassisted" protocol, Alice prepares an input state ρ which is transmitted through the unknown channel $\mathcal{E}_\theta$ and transformed into the unknown output state $\mathcal{E}_\theta(\rho)$ for Bob. Consider this process to be performed n times, so that Alice sends n copies $\rho^{\otimes n}$ and Bob receives $\mathcal{E}_\theta(\rho)^{\otimes n}$ assuming that the channel is memoryless. To retrieve θ, Bob applies an optimal generally-joint measurement to his n-copy output state. The type of measurement is different depending on the problem. In channel estimation, the measurement has a continuous outcome from which Bob constructs an unbiased estimator $\tilde{\theta}$ of θ, affected by some error variance $\delta\theta^2 := \langle(\tilde{\theta} - \theta)^2\rangle$. In channel discrimination, Bob uses a dichotomic measurement which provides the bit u with some mean error probability p_{err}.

The most general estimation/discrimination protocol is based on unlimited entanglement and adaptive quantum operations (QOs), which are applied jointly by Alice and Bob[12,27,31,32]. As also discussed in ref. 26, this protocol can be represented as a quantum comb[86]. This is a quantum circuit board whose slots are filled with the unknown quantum channel $\mathcal{E}_\theta$. The comb is based on a register with an arbitrary number of systems, prepared in some fundamental state ρ. The entire register undergoes arbitrary QOs before and after channel $\mathcal{E}_\theta$ is probed, as depicted in Fig. 1. The QOs can always be assumed to be trace-preserving by adding extra systems and adopting the principle of deferred measurement[1]. At the output of the comb, the state ρ_θ^n is detected by an optimal quantum measurement whose outcome is classically processed.

It is clear that the quantum comb encompasses the previous block protocol with output $\rho_\theta^n = \mathcal{E}_\theta(\rho)^{\otimes n}$. It also includes the "block-assisted" protocol where the input state is bipartite and comprises a signal system s, sent to probe the channel, and an idler or reference system r, which only assists the output measurement. By repeating the process n times, the output is given by $\rho_\theta^n = \mathcal{E}_\theta \otimes \mathcal{I}(\rho_{sr})^{\otimes n}$, where $\mathcal{I}$ is an identity channel. Finally, the comb can also describe "sequential" protocols where the input state is transmitted through n instances of the channel $\mathcal{E}_\theta \circ \cdots \circ \mathcal{E}_\theta$. See Fig. 1 for this classification.

Performance of channel estimation
Assume that the quantum comb in Fig. 1 is used and optimized for the problem of quantum channel estimation. Then, the ultimate performance is limited by the quantum Cramer Rao bound (QCRB)

$$\delta\theta^2 \geq \frac{1}{\mathrm{QFI}(\rho_\theta^n)}, \qquad (1)$$

where QFI is the quantum Fisher information[9]

$$\mathrm{QFI}(\rho_\theta^n) = \frac{8[1 - F(\rho_\theta^n, \rho_{\theta+d\theta}^n)]}{d\theta^2}, \qquad (2)$$

with $F(\rho, \sigma) := \mathrm{Tr}\sqrt{\sqrt{\sigma}\rho\sqrt{\sigma}}$ being the Bures fidelity between two states ρ and σ.

We are interested in the "scaling" of the QCRB, i.e., on how $\delta\theta^2$ behaves for large number of uses n. Here there are two main behaviors to consider. The first one is known as the standard quantum limit (SQL) which is the typical scaling $\delta\theta^2 \gtrsim n^{-1}$ achievable in classical strategies. The other is the Heisenberg limit $\delta\theta^2 \gtrsim n^{-2}$ which can only be achieved in a purely quantum setting. These have energy analogues when we consider continuous variable systems[5] and parameter estimation with bosonic channels. Assuming a single-use ($n = 1$) of the comb and an energy-constrained input state with N mean number of photons, then $\delta\theta^2 \gtrsim N^{-1}$ corresponds to the SQL, while $\delta\theta^2 \gtrsim N^{-2}$ is the Heisenberg limit.

For instance, the Heisenberg limit is achievable for large n when we estimate the phase factor φ of a unitary $U_\varphi = e^{i\varphi H}$ with H being the free Hamiltonian. In fact, it is sufficient to use the sequential protocol with an input pure state $|0, 1\rangle_{sr} + |1, 0\rangle_{sr}$ so that we have the output $|0, 1\rangle_{sr} + e^{in\varphi}|1, 0\rangle_{sr}$ where the phase coherently accumulates. The same limit is achievable in the number of photons N by using the N00N state $|N, 0\rangle_{sr} + |0, N\rangle_{sr}$ in a single use of the block-assisted protocol.

We know a simple criterion to establish if channel estimation is limited to the SQL. In particular, Pirandola and Lupo[27] shed light on the role of teleportation[87–89] in quantum metrology finding that the property of teleportation covariance[33] implies the SQL. Recall that a channel $\mathcal{E}$ is tele-covariant if, for any teleportation unitary U (Pauli[1] or displacement operator[5]), we may write[33]

$$\mathcal{E}(U\rho U^\dagger) = V\mathcal{E}(\rho)V^\dagger, \qquad (3)$$

for a generally different unitary V. Because of this property, a quantum channel is teleportation-simulable or Choi-stretchable, i.e., we may write the simulation[33,34]

$$\mathcal{E}(\rho) = \mathcal{T}(\rho \otimes \rho_\mathcal{E}), \qquad (4)$$

where $\mathcal{T}$ is the QO of teleportation and $\rho_\mathcal{E}$ is the channel's Choi matrix $\rho_\mathcal{E} := \mathcal{E} \otimes \mathcal{I}(\Phi_{sr})$, with Φ_{sr} being a maximally entangled state.

Here two observations are in order. First, let us remark that the simulation in Eq. (4) needs a suitable asymptotic formulation[33,34] for bosonic channels, whose Choi matrices are energy-unbounded. In fact, a bosonic channel $\mathcal{E}$ has Choi matrix $\rho_\mathcal{E} := \lim_\mu \rho_\mathcal{E}^\mu$, where the Choi sequence $\rho_\mathcal{E}^\mu := \mathcal{E} \otimes \mathcal{I}(\Phi_{sr}^\mu)$ is based on the two-mode squeezed vacuum (TMSV) state[5] Φ_{sr}^μ with variance $\mu = 2N + 1$, with N being the mean number of thermal photons in each mode. Second, let us note that a teleportation-covariant channel $\mathcal{E}$ is a specific type of programmable channel[28–31], where the quantum gate array is teleportation and the program state is the Choi matrix of the channel. The teleportation simulation has specific advantages in terms of achievability of the QCRB[26].

By definition, a parametrized quantum channel $\mathcal{E}_\theta$ is jointly teleportation-covariant[27] if we may write Eq. (3) for any θ, i.e., $\mathcal{E}_\theta(U\rho U^\dagger) = V\mathcal{E}_\theta(\rho)V^\dagger$, so that the output unitary V depends on U but not on θ. Because of
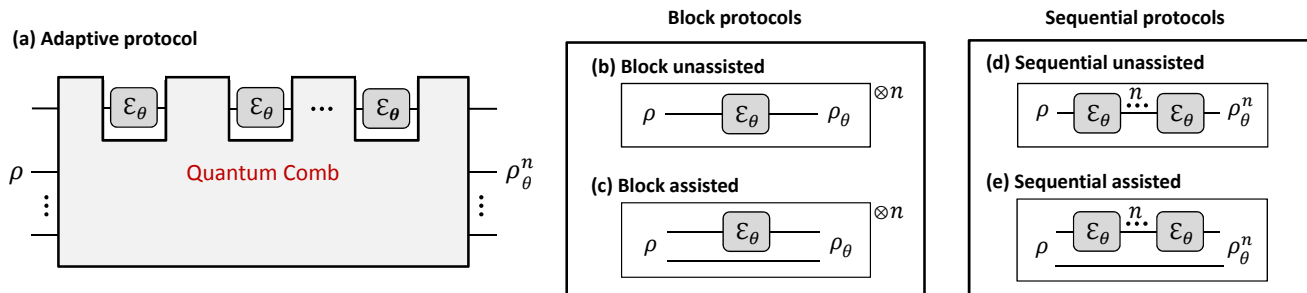
FIG. 1: Protocols for quantum estimation and discrimination. **(a)** Adaptive protocol represented as a quantum comb. An input register with an arbitrary number of systems (wires) is prepared in a fundamental initial state ρ. Each probing of the unknown channel $\mathcal{E}_\theta$ is performed by inputting a system from the register and storing the output back in the register. Probings are interleaved by arbitrary QOs performed over the entire register. After n probings, the total output ρ_θ^n is subject to a joint quantum measurement. **(b)** Block unassisted protocol where channel $\mathcal{E}_\theta$ is probed n times in an identical and independent way. **(c)** Block assisted protocol where channel $\mathcal{E}_\theta$ is probed by a signal system coupled to a reference system. **(d)** Sequential unassisted protocol where the input is transmitted through n consecutive instances of the channel $\mathcal{E}_\theta$. **(e)** Sequential assisted protocol where the input is bipartite and partially transmitted through n consecutive instances of $\mathcal{E}_\theta$.

this property, we may write the teleportation simulation $\mathcal{E}_\theta(\rho) = \mathcal{T}(\rho \otimes \rho_{\mathcal{E}_\theta})$ for any θ. Replacing this simulation in each slot of the quantum comb in Fig. 1 and "stretching" the adaptive protocol, we write the output state as

$$\rho_\theta^n = \Lambda(\rho_{\mathcal{E}_\theta}^{\otimes n}), \qquad (5)$$

for a global quantum channel Λ. Because the QFI is monotonic under channels and multiplicative over tensor products, one finds that $\text{QFI}(\rho_\theta^n) \leq n\text{QFI}(\rho_{\mathcal{E}_\theta})$, so that the QCRB must satisfy the SQL

$$\delta\theta^2 \geq [n\text{QFI}(\rho_{\mathcal{E}_\theta})]^{-1}, \qquad (6)$$

where we implicitly mean $\text{QFI}(\rho_{\mathcal{E}_\theta}) := \lim_\mu \text{QFI}(\rho_{\mathcal{E}_\theta}^\mu)$ for a bosonic channel. In other words, the adaptive protocol has been reduced to a block assisted protocol, where n maximally-entangled states $\Phi_{sr}^{\otimes n}$ are used to probe the unknown quantum channel $\mathcal{E}_\theta$.

Because the class of teleportation-covariant channels is wide, we have that channel estimation is limited to the SQL in many situations. For instance, the estimation of the probability parameter p in depolarizing, dephasing or erasure channels is limited to[27] $\delta p^2 \geq p(1-p)n^{-1}$. Then, the estimation of the thermal noise $\bar{n}$ in a thermal-loss channel $\mathcal{E}_{\eta,\bar{n}}$ with fixed transmissivity η is limited to[27] $\delta\bar{n}^2 \geq \bar{n}(\bar{n}+1)n^{-1}$, which sets the limit for estimating excess noise in quantum key distribution. By contrast, the ultimate estimation limit for the transmissivity η is not known. Because $\mathcal{E}_{\eta,\bar{n}}$ is not jointly teleportation-covariant in η, the reduction in Eq. (6) does not apply.

The optimal estimation of bosonic loss is an open problem with a number of partial results. Solving this problem is important because loss is the main decoherence effect in quantum optical communications, from fibre-based to free-space implementations. Recall that the transmissivity η limits the ultimate rate achievable by point-to-point protocols of quantum and private communication according to the Pirandola-Laurenza-Ottaviani-Banchi bound[33], so that $-\log_2(1-\eta)$ bits per use cannot

be exceeded without repeaters. Estimating η is therefore of paramount importance. The best-known performance in estimating the transmissivity η of a pure-loss channel $\mathcal{E}_\eta := \mathcal{E}_{\eta,0}$ is limited to the SQL $\delta\eta^2 \geq \gamma N^{-1}$, with a pre-factor γ which has been improved over time.

Monras and Paris[90] studied the block unassisted protocol with single-mode Gaussian states. They established the limit $\delta\eta^2 \geq \eta N^{-1}$ achievable by using coherent-states, also known as shot-noise limit or classical benchmark. They also found that squeezing may improve the pre-factor and, therefore, beat the shot-noise limit. These results may be achieved by computing the QFI as in Eq. (2) and using the formulas for the fidelity between Gaussian states[91]. The best performance so far has been achieved by using the block protocol with non-Gaussian states, including Fock states. In this way, Adesso et al.[92] found the improved scaling $\delta\eta^2 \geq \eta(1-\eta)N^{-1}$.

Performance of channel discrimination
Now assume that the quantum comb in Fig. 1 is used and optimized for binary discrimination, i.e., for the retrieval of the parameter θ from a binary alphabet $\{\theta_0, \theta_1\}$ where the two possible values have identical Bayesian cost and the same prior probability. This is now a problem of quantum channel discrimination, where we aim at distinguishing between two channels $\mathcal{E}_0 = \mathcal{E}_{\theta_0}$ and $\mathcal{E}_1 = \mathcal{E}_{\theta_1}$, or equivalently at retrieving the classical bit u from $\mathcal{E}_u$. Let us call ρ_0^n and ρ_1^n the two possible output states of the comb. The optimal performance in terms of the minimum error probability is given by the Helstrom bound[16]

$$p_{\text{err}}(\mathcal{E}_0, \mathcal{E}_1) = [1 - D(\rho_0^n, \rho_1^n)]/2, \qquad (7)$$

where $D(\rho, \sigma) := ||\rho - \sigma||/2$ is the trace-distance[1]. This is obtained by a suitable dichotomic positive-operator valued measure (POVM), called Helstrom POVM. Equivalently, note that the maximum classical information J retrieved from the box is equal to

$$J = 1 - H_2[p_{\text{err}}(\mathcal{E}_0, \mathcal{E}_1)], \qquad (8)$$

where H_2 is the binary Shannon entropy.

The error probability greatly simplifies if the two channels $\mathcal{E}_0$ and $\mathcal{E}_1$ are jointly teleportation-covariant, i.e., we may write $\mathcal{E}_u(U\rho U^\dagger) = V\mathcal{E}_u(\rho)V^\dagger$ for any u. This allows us to use the teleportation simulation $\mathcal{E}_u(\rho) = \mathcal{T}(\rho \otimes \rho_{\mathcal{E}_u})$ over the Choi matrix $\rho_{\mathcal{E}_u}$. We may then stretch the comb and write its output as $\rho_u^n = \Lambda(\rho_{\mathcal{E}_u}^{\otimes n})$ for a global channel Λ. Because the trace distance is monotonic under Λ, we have $p_{\mathrm{err}} \geq [1 - D(\rho_{\mathcal{E}_0}^{\otimes n}, \rho_{\mathcal{E}_1}^{\otimes n})]/2$. Now note that this is achievable by an assisted protocol which exploits maximally-entangled states at the input, so that[27]

$$p_{\mathrm{err}}(\mathcal{E}_0, \mathcal{E}_1) = [1 - D(\rho_{\mathcal{E}_0}^{\otimes n}, \rho_{\mathcal{E}_1}^{\otimes n})]/2, \qquad (9)$$

where $D = \lim_\mu D(\rho_{\mathcal{E}_0}^{\mu\otimes n}, \rho_{\mathcal{E}_1}^{\mu\otimes n})$ for bosonic channels. In finite dimension, Eq. (9) implies that the diamond distance between two jointly teleportation-covariant channels is simply equal to $||\mathcal{E}_0 - \mathcal{E}_1||_\diamond = ||\rho_{\mathcal{E}_0} - \rho_{\mathcal{E}_1}||$.

Starting from Eq. (9), we may write simple lower and upper bounds using the Fuchs-van de Graaf relations[93] and the quantum Chernoff bound (QCB)[20]. In fact, recall that for any pair of multicopy states $\rho_0^{\otimes n}$ and $\rho_1^{\otimes n}$, the minimum error probability $p_{\mathrm{err}} = [1 - D(\rho_0^{\otimes n}, \rho_1^{\otimes n})]/2$ satisfies the fidelity-based lower bound and the QCB

$$p_{\mathrm{err}} \geq \frac{1 - \sqrt{1 - F(\rho_0, \rho_1)^{2n}}}{2} := F_-^{(n)}(\rho_0, \rho_1), \qquad (10)$$

$$p_{\mathrm{err}} \leq \frac{Q(\rho_0, \rho_1)^n}{2}, \quad Q := \inf_s \mathrm{Tr}(\rho_0^s \rho_1^{1-s}). \qquad (11)$$

In particular, for multimode Gaussian states, ρ_0 and ρ_1, we know closed formulas for computing the fidelity[91] and the QCB[22]. These inequalities can be extended to the adaptive error probability of Eq. (9) valid for jointly teleportation-covariant channels, so that we may write[27]

$$F_-^{(n)}(\rho_{\mathcal{E}_0}, \rho_{\mathcal{E}_1}) \leq p_{\mathrm{err}}(\mathcal{E}_0, \mathcal{E}_1) \leq \frac{Q(\rho_{\mathcal{E}_0}, \rho_{\mathcal{E}_1})^n}{2}, \qquad (12)$$

with asymptotic functionals over bosonic Choi matrices.

The results in Eqs. (9) and (12) apply to many cases, including the adaptive discrimination of Pauli channels, erasure channels, and the noise parameters in bosonic Gaussian channels, such as the thermal photons $\bar{n}_0$ and $\bar{n}_1$ in thermal-loss channels $\mathcal{E}_{\eta,\bar{n}_0}$ and $\mathcal{E}_{\eta,\bar{n}_1}$ with the same transmissivity η. Unfortunately, the same reduction does not apply to the discrimination of bosonic loss, e.g., η_0 and η_1 of a thermal-loss channel with fixed noise $\bar{n}$, because $\mathcal{E}_{\eta_0,\bar{n}}$ and $\mathcal{E}_{\eta_1,\bar{n}}$ are not jointly teleportation-covariant. As a result, establishing the optimal discrimination of bosonic loss is still an open problem. What we know currently is that block-assisted strategies based on entangled states may greatly outperform block unassisted strategies, especially when we employ a small number of signal photons in the presence of thermal noise. This is the observation which is at the basis of the applications of quantum reading and quantum illumination.

Quantum reading of classical data
In 2011, ref. 35 showed how the readout of classical data from an optical digital memory can be modelled as a problem of quantum channel discrimination. In the most basic description, an optical classical memory can be seen as an array of cells described as microscopic beamsplitters with different reflectivities (see Fig. 2). Each cell stores an information bit $u = 0, 1$ in two equiprobable reflectivities, the pit-reflectivity $\eta_0 \in (0, 1)$ and the land-reflectivity $\eta_1 > \eta_0$. This single-cell model is equivalent to a black-box model read in reflection so that the reflectivity plays the role of the transmissivity parameter. The readout may also be affected by thermal noise, e.g., due to stray photons generated by the source. Thus the readout corresponds to discriminating between two thermal-loss channels, $\mathcal{E}_0 := \mathcal{E}_{\eta_0,\bar{n}}$ and $\mathcal{E}_1 := \mathcal{E}_{\eta_1,\bar{n}}$, with different reflectivity, η_0 and η_1, but fixed thermal number $\bar{n}$. Other decoherence effects may be included[35], such as optical diffraction, memory effects and inter-bit interference[36].

We may consider different "transmitters" composed of signal modes probing the cell and reference modes assisting detection. The coherent-state transmitter only uses n signal modes in identical coherent states $|\alpha\rangle_s \langle\alpha|^{\otimes n}$. More powerfully, we may define a "classical" transmitter in the quantum optical sense[94,95]. This is a block assisted protocol employing mixtures of coherent states $\int d^{2n}\alpha \, \mathcal{P}(\alpha)|\alpha\rangle\langle\alpha|$, where $\mathcal{P}(\alpha)$ is a probability distribution of amplitudes α, and $|\alpha\rangle\langle\alpha|$ is a multimode coherent state with n signal modes and n reference modes. The optimal classical transmitter has to be compared with an Einstein-Podolsky-Rosen (EPR) transmitter. This is a block entanglement-assisted protocol where we send part of n TMSV states $\Phi_{sr}^{\mu\otimes n}$, so that each signal mode is entangled with a reference or "idler" mode.

For both the classical and the EPR transmitter, we therefore assume an input $2n$-mode state ρ_{sr}, which is transformed by the cell into an output state $\sigma_u := \mathcal{E}_u^{\otimes n} \otimes \mathcal{I}^{\otimes n}(\rho_{sr})$ for the n reflected signal modes and the n kept reference modes. This output is detected by an optimal Helstrom POVM with some error probability. We then compare the optimal information retrieved by the classical transmitter J_{class} with that retrieved by the EPR transmitter J_{EPR}, quantifying the information gain $\Delta := J_{\mathrm{EPR}} - J_{\mathrm{class}}$. Positive values $\Delta > 0$ provide quantum advantage. A fair comparison between these transmitters involves fixing the mean number of signal photons probing the cell. Because each cell is probed n times, we may consider different types of energy constraints.

One type of constraint is "local", meaning that we fix the mean number of photons N in each probing, so that the total energy scales as nN. We may write the following general bound for the error probability p_{class} achievable by any classical transmitter[35]

$$p_{\mathrm{class}} \geq \mathcal{C}(n, N) := \frac{1 - \sqrt{1 - F(N)^{2n}}}{2}, \qquad (13)$$

where $F(N)$ is Bures fidelity between the two possible outputs $\mathcal{E}_0(|\sqrt{N}\rangle\langle\sqrt{N}|)$ and $\mathcal{E}_1(|\sqrt{N}\rangle\langle\sqrt{N}|)$ generated by a single-mode coherent state with N mean photons. This leads to the upper bound $J_{\mathrm{class}}(n, N) \leq 1 - H_2[\mathcal{C}(n, N)]$. For the EPR transmitter, we may exploit the QCB which
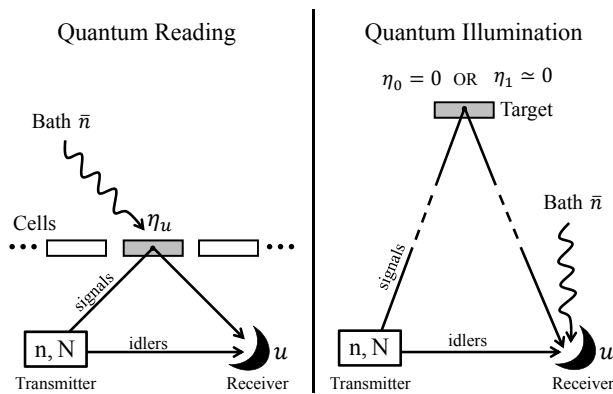
FIG. 2: Quantum reading (left) and Gaussian quantum illumination (right). In the basic formulation, these are both based on an EPR transmitter, so that n two-mode squeezed vacuum (TMSV) states irradiate N mean photons per mode over the cell/target (where N is typically low). The reflected signals are combined with the retained idler (reference) modes in a joint detection, whose output u discriminates between two hypotheses. In quantum reading, u is the information bit encoded into a cell with reflectivity η_u and subject to thermal noise $\bar{n}$. In quantum illumination, u is related with the absence ($\eta_0 = 0$) or the presence ($\eta_1 \simeq 0$) of a low-reflectivity target. The reflection is mixed with an environment with bright thermal noise $\bar{n} \gg 1$. These schemes are examples of block-assisted protocols for quantum channel discrimination. In the regimes considered, they largely outperform classical strategies, i.e., corresponding schemes based on classical transmitters that are not entangled but composed of mixtures of coherent states.

gives the lower bound $J_{\text{EPR}} \geq 1 - H_2[Q(\rho^\mu_{\mathcal{E}_0}, \rho^\mu_{\mathcal{E}_1})^n/2]$, where $\rho^\mu_{\mathcal{E}_u}$ is the quasi-Choi matrix of the unknown channel $\mathcal{E}_u$ probed by a TMSV state Φ^μ_{sr} with $\mu = 2N + 1$. Using these bounds we construct a sufficient condition to prove the quantum advantage $\Delta > 0$.

Numerical investigations show that positive values of Δ are typical for low signal photons and high reflectivities in wide ranges for the thermal noise. A positive quantum advantage can already be achieved by a single probe per cell ($n = 1$). When the land-reflectivity is very high $\eta_1 \to 1$ (ideal memory), one may derive analytical expressions[37] and find regimes of parameters for which $\Delta \to 1$ bit per cell. This extremal value means that the EPR transmitter is able to fully read the cell, while classical transmitters do not retrieve any information. This advantage may also be used to design cryptographic memories whose data can only be read by entanglement[38].

Another type of energy constraint is "global", meaning that we fix the total mean number of photons N_T over all the n uses, so that we employ an average of N_T/n photons per probing. Let us call n the bandwidth of the transmitter, due to the fact that this can be physically related with the number of effective frequencies used in the readout. One can then show that, at sufficiently low energies $N_T \lesssim 10$ photons, a narrowband EPR transmitter (even monochromatic $n_{\text{EPR}} = 1$) is able to beat arbitrary

classical transmitters, up to extremely large bandwidths. Because a few entangled photons can retrieve more information than any classical source of light, we may indeed work at very low energies. This regime may be mapped into much faster optical readers and denser memories[35].

Quantum reading has been extensively studied[39–49]. Ref. 39 extended the model to multi-cell error correction coding and defined the notion of quantum reading capacity, a quantity that was later shown to be super-additive[40]. Guha and Shapiro[41] also defined a similar notion of capacity[42] and studied the error exponent for quantum reading. For single-cell reading of an ideal memory in noiseless conditions, Nair[43] showed that Fock states are optimal. More generally, entangled states with the signal beam in a number-diagonal reduced state may also provide a positive quantum advantage[43]. This class of states is optimal for non-adaptive discrimination with single-mode and multi-mode pure-loss channels[44].

Hirota[45] proposed an alternative model based on a binary phase encoding and showed how entangled coherent states may achieve error-free quantum reading. Non-Gaussian entangled states were also considered by Prabhu Tej et al.[46]. Then, Bisio et al.[47] studied a noise-free unitary model of quantum reading where both the inputs of the unknown beamsplitter are accessible for probing and both its outputs for detection. Assuming a single probe ($n = 1$), they found that the optimal two-mode input is the superposition of a N00N state and the vacuum $|00\rangle$. This approach was later extended by Dall'Arno et al.[48] to unambiguous quantum reading, where the probability of error is replaced by an inconclusive result.

Similar to Hirota[45], Dall'Arno et al.[48] also considered a version of perfect quantum reading with zero discrimination error. This is possible by designing an ideal cell which is either a beamsplitter with perfect reflectivity ($\eta_1 = 1$) or a beamsplitter with lower reflectivity $\eta_0 < 1$ and suitable $\pm\pi/2$ phase shifters at the input and output ports. This scheme was experimentally implemented[48]. As shown in Fig. 3(a), the setup consisted of a Mach-Zehnder interferometer with the variable beamsplitter situated in one arm. A heralded single photon source based on spontaneous parametric down-conversion in a 2mm long beta barium borate (BBO) crystal pumped with a continuous-wave laser diode at 405nm served as the quantum state source. The photon pairs generated in orthogonal polarizations in the type-II phase matching process were separated by a polarizing beamsplitter. While one photon was used to herald the process, the other was fed into the Mach-Zehnder interferometer.

The setup discriminated between two beamsplitter configurations, the one with reflectivity $\eta_1 = 1$ and the other with reflectivity $\eta_0 < 1$ and an additional phase shift in the Mach-Zehnder interferometer arm. The measurement consisted of three photon counters, one at the output of the variable beamsplitter under test and the other two at each output of the interferometer. Coincidence counts between each of the three detectors and the trigger detector were measured using a 3ns coinci-

dence window. With the perfect beamsplitter under test, only one of the detectors at the output of the Mach-Zehnder interferometer would detect the photon (Hong-Ou-Mandel effect), while for the beamsplitter with $\eta_0 < 1$ then any of the two other detectors would detect the photon (due to the additional phase shift).

Quantum illumination of targets

Quantum sensing can be used not only to enhance the readout of information from classical systems, but also to boost the standoff detection of remote objects. This idea was first pushed forward by the efforts of Lloyd and Shapiro at MIT[50–52]. In 2008, Lloyd[50] designed a qubit-based protocol of quantum illumination, showing how the detection of a low-reflectivity target object can be enhanced by using quantum entanglement. The advantage of the entangled transmitter over non-entangled ones is achieved even if the entanglement itself is completely lost after reflection from the target. In fact, the initial signal-idler entanglement is mapped into residual but yet quantum correlations between the reflected signal and the kept idler that a suitably-designed quantum detector may "amplify" with respect to the uncorrelated thermal background.

In the same year, Shapiro's team[51] proposed a practical formulation of quantum illumination based on continuous-variable systems[5]. Ref. 51 designed a Gaussian version where bosonic modes are prepared in Gaussian states and sent to detect an object with low reflectivity $\eta \simeq 0$ in a region with bright thermal noise, i.e., with $\bar{n} \gg 1$ mean thermal photons. The detection process can be modelled as the discrimination between a zero-reflectivity thermal-loss channel $\mathcal{E}_{\eta=0,\bar{n}}$ (target absent) and a low-reflectivity thermal-loss channel $\mathcal{E}_{\eta,\bar{n}'}$ with $\eta \simeq 0$ and $\bar{n}' = \bar{n}/(1-\eta)$ (target present). Here the factor $(1-\eta)^{-1}$ excludes the possibility of a "passive signature" which means the possibility of detecting the target without transmitting any radiation by just measuring a lower received background level. As also depicted in Fig. 2, one assumes that the detector's noise does not depend on the presence of the target.

In this setup, we assume a local energy constraint, so that N mean photons are irradiated by each of the n bosonic modes sent over the target object. Under this assumption, we compute the error probability associated with the various transmitters. In particular, we exploit the bounds in Eqs. (10) and (11) to compare the performance of the EPR transmitter (based on TMSV states) with that of the classical transmitter (based on coherent states). In the regime of low-energy signals ($N \ll 1$) and many modes ($n \gg 1$), the EPR transmitter has the scaling[51] $p_{\text{EPR}}^{\text{err}} \simeq \exp(-n\eta N/\bar{n})/2$, which clearly beats the classical transmitter $p_{\text{class}}^{\text{err}} \geq \exp(-n\eta N/2\bar{n})/4$. In particular, $p_{\text{EPR}}^{\text{err}}$ realizes a 6dB advantage in the error-probability exponent over the coherent-state transmitter $p_{\text{CS}}^{\text{err}} \simeq \exp(-n\eta N/4\bar{n})/2$. Zhuang et al.[53] proved that the theoretical limit $p_{\text{EPR}}^{\text{err}}$ can be achieved by an explicit quantum receiver based on feed-forward sum-frequency generation. This receiver has been also used to show the

quantum illumination advantage in terms of detection probability versus false-alarm probability[54].

In 2015, Gaussian quantum illumination was extended to the microwave regime, thus providing a prototype of quantum radar[55]. In this scheme, an electro-optomechanical converter[97–99] transforms an optical mode into microwave. If this transducer has high quantum efficiency, then optical-optical entanglement is translated into microwave-optical entanglement. The microwave signal is sent to probe the target region, while the optical idler is retained. The microwave radiation collected from the target region is then phase conjugated and upconverted into an optical field by a second use of the transducer. The optical output is finally combined with the retained idler in a joint detection, following the ideas behind the receiver design by Guha and Erkmen[56]. In this way, ref. 55 found that the error probability of microwave quantum illumination is superior to that of any classical radar of equal transmitted energy. A followup analysis has been carried out by Xiong et al.[57].

More recently, Sanz et al.[58] studied the protocol of quantum illumination using the tools of quantum metrology so as to measure the reflectivity of the target. They employed the QFI to bound the error probability showing a 3dB-enhancement of the signal-to-noise ratio with respect to the use of local measurements. They also considered non-Gaussian Schrödinger's cat states. Other studies have quantified the quantum illumination advantage in terms of "consumption" of discord[96] associated with the target[59], and in terms of mutual information[60]. Finally note that quantum illumination has been also studied as an asymmetric Gaussian discrimination problem by various authors[25,54,61,62]. In this setting, TMSV states have been identified as optimal probes[62]. Finding the ultimate performance achievable by an *adaptive* version of quantum illumination remains an open question.

Several experimental implementations of quantum illumination have been reported[63,65,66]. As depicted in Fig. 3(b), Lopaeva et al.[63] exploited a parametric down-conversion source using a BBO crystal to generate two intensity-correlated light beams in orthogonal polarizations at 710nm. Both beams were detected by a photon-counting high-quantum efficiency CCD camera. The target object, a 50:50 beamsplitter in the experiment, was placed in one of the two entangled beams before detection. The beamsplitter object was illuminated by photons scattered on an Arecchi's rotating ground glass to simulate a thermal environment. A single captured image was used to measure the second-order correlations between the two beams. The implementation shows robustness against noise and losses, and demonstrates a quantum enhancement in target detection in thermal environments even when nonclassicality is lost. However, coincidence detection of spontaneous parametric down-conversion is not the optimal detection method to extract the most information from the signal-idler entangled modes, and the implemented classical scheme using weakly thermal states is also non-optimal.
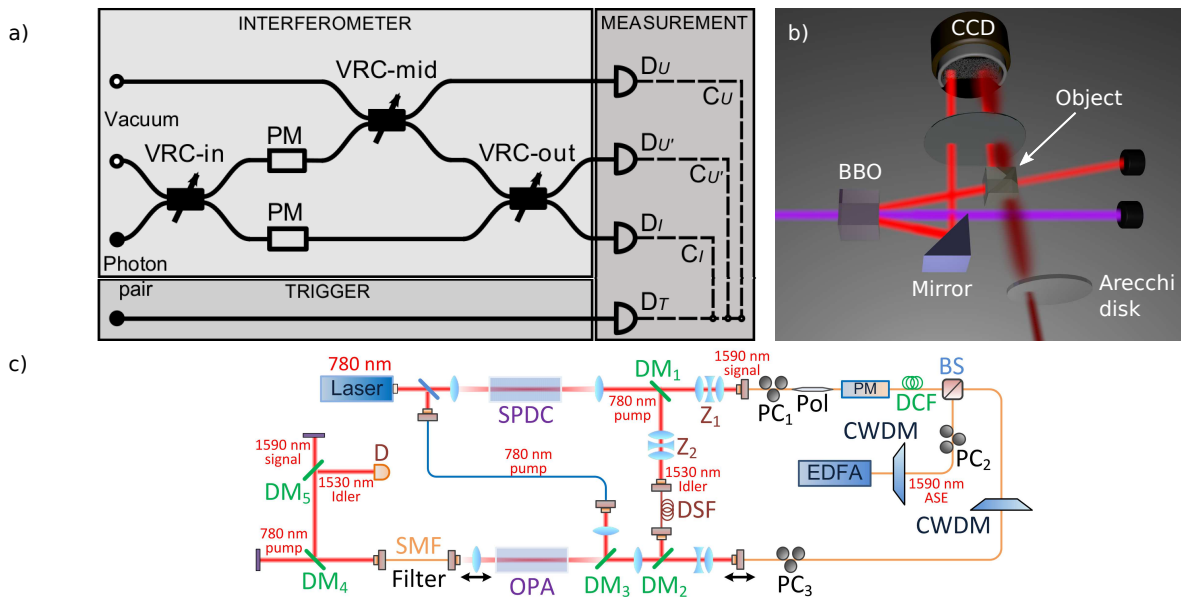
FIG. 3: Experimental demonstrations of quantum reading and quantum illumination. **a)** Experimental setup of perfect quantum reading[48]. A photon pair source is used to generate a heralded single photon using a trigger detector (D_T). The heralded single photon is fed into an interferometer with variable ratio couplers (VRCs) and phase modulators (PMs) to add additional phase shifts. Coincidence detection of the outputs are used to discriminate between two possible splitting ratios of VRC-mid. **b)** Quantum illumination experiment of Lopaeva et al.[63]. See also Ref. 64. Both beams of a photon pair source are detected by a photon counting CCD camera. In the experiment the target is a 50:50 beamsplitter placed in one of the beams. The beamsplitter is simulated to be in a thermal environment by illuminating it with scattered light from an Arrechi disk. **c)** Quantum illumination experiment of Zhang et al.[66]. Photon pairs generated by spontaneous parametric down-conversion (SPDC) at two different wavelengths are split using a dichroic mirror (DM). One of the photons is stored in a delay line using a dispersion-shifted LEAF fiber (DSF). The other photon is phase modulated (PM). A lossy and noisy environment is simulated by a beamsplitter (BS) and amplified spontaneous emission (ASE) from a erbium doped fiber amplifier (EDFA). The joint detection is implemented using an optical parameteric amplifier (OPA) whose output is detected by a PIN photo detector (D). DCF: dispersion-compensating fiber, POL: polarizer, CWDM: coarse wavelength-division multiplexer. Thin lines are optical fiber, thick lines are unguided propagation. Figures adapted with permission from: a), ref. 48, © 2012 APS; b), ref. 63, © 2013 APS; c) ref. 66, © 2015 APS.

Adopting a different approach, in 2013 Zhang et al.[65] reported a secure communication experiment based on quantum illumination. More recently, Zhang et al.[66] demonstrated the advantage of quantum illumination over coherent states by using broadband entangled Gaussian states, as produced by continuous-wave spontaneous parametric down-conversion. In the experiment shown in Fig. 3(c), the signal modes were phase modulated before probing the weakly-reflecting target, while the idler modes were stored in a delay line. The joint measurement was performed by combining the reflected signal modes and the idler modes with a pump in another optical parametric amplifier. The output in the order of nW was then detected by a PIN photo detector with high gain and low noise. They showed a 20% improvement of the signal-to-noise ratio in comparison to the optimal classical scheme in an environment exhibiting 14dB loss and a thermal background 75dB above the returned probe light.

Optical resolution beyond the Rayleigh limit
The Rayleigh criterion is a well-known result in classical imaging. Two point-like sources cannot be optically resolved (in the far field) if they are closer than the Rayleigh length $\simeq \lambda/a$, where λ is the wavelength of the emitted light and a is the numerical aperture of the observing lens. For this reason, if we use a converging optical system to focus light on a screen and an array of detectors to measure the intensity, the Rayleigh's criterion together with the presence of photon shot noise, can lead to severe limitations in resolving point-like sources. The situation changes completely if we consider a fully quantum description of the light and the measurement apparatus. In this way, Tsang et al.[69] showed the existence of a quantum detection scheme able to measure the distance between two point-like sources with a constant accuracy, even when the sources have sub-wavelength separation. This ground-breaking result was achieved by relating the problem of resolving two incoherent point-like sources to quantum estimation theory and using the QCRB.

The theory beyond these results were extended from incoherent sources emitting faint pulses to thermal sources of arbitrary brightness[70,71]. In general, ref. 70 established a connection between optical resolution and bosonic channel estimation, so that measuring the separation between two point-like sources is equivalent to

estimating the loss parameters of two lossy channels. In this way, ref. 70 developed a theory of super-resolution for point-like sources emitting light in a generic state, i.e., attenuated or bright, classical, coherent, incoherent, as well as entangled (e.g., in a microscope setup). The ultimate resolution was found as a function of the optical properties of the two sources and their separation. In particular, super-resolution can be enhanced when the sources emit entangled or quantum-correlated (discordant) light.

More recently, Kerviche et al.[72] extended Tsang et al.'s analysis from a Gaussian point spread function to a hard-aperture pupil, proving the information optimality of image-plane sinc-Bessel modes. They also generalized the result to an arbitrary point spread function. Rehacek et al.[73] carried out further work on the optimal measurements for beating the Rayleigh limit. Yang et al.[74] explored the use of homodyne or heterodyne detection. Finally, Lu et al.[75] studied the quantum-optimal detection of one-versus-two incoherent optical sources with arbitrary separation.

Shortly after the idea of Tsang et al.[69] was presented, it was experimentally verified in several proof-of-principle experiments. The first experiment by Tang et al.[76] was based on super-localization by image inversion interferometry[77]. As shown in Fig. 4(a), they used an image inversion interferometer to determine the separation of two incoherent point sources, generated by two laser beams in orthogonal polarizations stemming from the same HeNe laser. Using the light from the simulated sources as the input, the interferometer was implemented as a Mach-Zehnder interferometer with image inversion generated by a lens system in one arm. The other arm was delayed appropriately so that the detector at the output of the interferometer ideally showed no response for zero separation due to destructive interference. With growing separation of the two sources the destructive interference becomes more and more imperfect, yielding an optical resolution beyond the Abbe-Rayleigh limit.

Yang et al.[78] used heterodyne detection with a local oscillator in TEM01 mode to detect the separation of the two slits in a double slit configuration beyond the classical resolution limit. As also depicted in Fig. 4(b), they use a piece of paper to achieve incoherence and diffuse transmission. Measuring at a frequency of some MHz to avoid noise at lower frequencies, the beat between the local oscillator and the beam illuminating the slits becomes zero if the separation is 0 as both spatial parts of the TEM01 mode have a phase shift of π. Separating the two slits yields a measurement beyond the Abbe limit. While the scheme requires the two sources to be exactly aligned to the center of the TEM01 mode, using higher-order TEM modes will provide general sub-Rayleigh imaging.

In another experiment, Tham et al.[79] inserted a phase shift of π into the beam resembling the two incoherent sources (generated by partially overlapping two beams in orthogonal polarizations) and projecting it onto the guiding mode of a single mode fiber, as in Fig. 4(c). Finally,

Paúr et al.[80] simulated Gaussian and slit apertures by a digital micromirror chip illuminated by a laser. Projection onto different modes was performed by a spatial light modulator which creates a digital hologram measured by an electron-multiplying CCD. See Fig. 4(d). Let us conclude that super-resolving quantum imaging is a hot topic and many other experiments could be mentioned[81–83].

Discussion and outlook

Quantum sensing is a rapidly evolving field with many potential implications and technological applications. Despite the great advances that have been achieved in recent years, a number of problems and experimental challenges remain open. From the point of view of the basic theoretical models of quantum metrology and quantum hypothesis testing, we may often compute the ultimate performances allowed by quantum mechanics. However, we do not know in general how to implement the optimal measurements achieving these performances and/or what optimal states we need to prepare at the input of the unknown quantum channel. Then, do we need to consider feedback and perform adaptive protocols? For instance, this is an open question for both estimation and discrimination of bosonic loss[26], which is at the basis of quantum reading, quantum illumination and quantum-enhanced optical super-resolution.

From a more practical and experimental point of view, there are non-trivial challenges as well. Despite a first proof-of-principle demonstration[48] based on the unitary discrimination of beamsplitters, we do not have yet a truly quantum reading experiment where a single output of the cells is effectively accessed for the readout. A full demonstration would involve an actual (one- or two-dimensional) array of cells, where information is stored with classical codes and the quantum readout is performed by simultaneously probing blocks of cells. This idea may be further developed into a full experiment of bosonic quantum pattern recognition where the use of entanglement across an array may boost the resolution of unsupervised problems of data clustering.

Quantum illumination has had various experimental demonstrations[63,65,66] but still remain the issue of designing a practical receiver that would allow one to closely approximate the theoretical limit forseen by the Helstrom bound. Challenges become more serious when we consider the implementation of quantum illumination in the microwave regime[55]. Here the development of highly-efficient microwave-optical quantum converters could mitigate experimental issues related with the generation of microwave entanglement and the detection of microwave fields at the single-photon level. Furthermore these converters are highly desired for other applications, in particular as interfaces for connecting superconducting quantum chips and optical fibers in a potential hybrid design of a future quantum Internet[89].

It is clear that other designs of a quantum radar are possible. For instance, a fully microwave implementation of quantum illumination (without the use of converters) may be achieved by using a superconducting Josephson
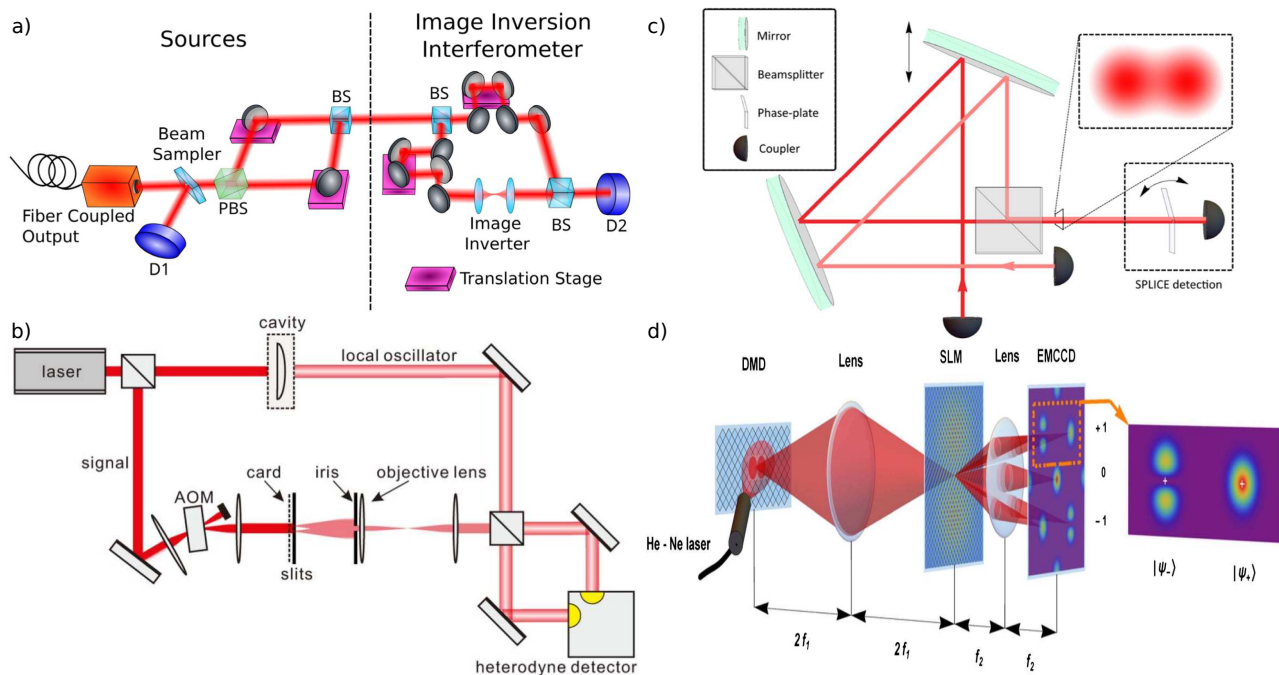
FIG. 4: Proof-of-principle experiments demonstrating a quantum detection scheme able to measure a distance of two incoherent point sources better than the Rayleigh limit. **a)** Experiment of Tang et al.[76]. A HeNe laser with fiber coupled output is split at a polarizing beamsplitter (PBS) into two beams of orthogonal polarization. They are recombined at a beamsplitter (BS) with a slight lateral displacement to simulate two incoherent light sources. The light sources are imaged using an image inversion interferometer, a Mach-Zehnder interferometer with an image inverter consisting of two lenses in one arm. One output of the interferometer is detected by a photo detector (D2). **b)** Experiment of Yang et al.[78]. The signal beam is frequency shifted by an acousto-optical modulator (AOM) and illuminates slits. A paper card is placed in front of the slits to make the illumination incoherent. The signal beam is measured by heterodyne detection using a local oscillator prepared in TEM01 mode by means of an optical cavity. **c)** Experiment of Tham et al.[79]. Two partially overlapping beams as shown in the upper inset are generated by coupling laser light out of a fiber and combining them on a beamsplitter. The distance between the beams can be controlled by the position of the upper mirror. The separation of the two beams is detected by projecting the beams onto a mode orthogonal to TEM00, in their case a spatially antisymmetric field mode. This is performed by passing the two beams through a phase plate which is built in such a way that it introduces different phase shifts between opposite halves of the beam and aligned such that coupling into a well-aligned fiber coupler is minimized. The coupling into a single mode fiber corresponds to a projection onto the TEM00 mode, thus together with the phase plate the beams are projected onto a mode orthogonal to TEM00. **d)** Experiment of Paúr et al.[80]. Using a high frequency switched digital micro mirror chip (DMD) illuminated by a HeNe laser two closely spaced incoherent beams are generated. The beam is projected onto different modes by an amplitude spatial light modulator (SLM) generating a digital hologram. The first-order diffraction spectrum is detected by an electron multiplying CCD (EMCCD) camera. Figures adapted with permission from: a), ref. 76, © 2016 OSA; b), ref. 78, © 2016 OSA; c) ref. 79, © 2017 APS; d) ref. 80, © 2016 OSA.

parametric amplifier to generate signal-idler microwave entanglement. Reflected signals could then be phase-conjugated via another parametric amplifier, recombined with the idlers, and finally measured, e.g., by using a transmon qubit as single-photon detector. The idea of using Josephson mixers and photocounters has been also studied by Las Heras et al.[67] in the context of using microwave quantum illumination to reveal phase-shift inducing cloaking, also known as "invisible cloak".

Other experimental challenges need to be addressed in order to build an actual quantum radar[68]. An important aspect is the preservation of the idler modes while the signals are being propagated forward and back from the target. The idlers should be kept in a low-loss delay line or stored in quantum registers with sufficiently-long coher-

ence times, until the final joint detection. Then, unlike classical radars, whose performance improves as the signal power is increased at constant bandwidth, the quantum counterpart needs to increase bandwidth at constant signal brightness. The challenge is therefore to generate microwave pulses with a time-bandwidth product of 10^6 modes or more. Furthermore, classical radars can interrogate many potential target bins with a single pulse, while present models of quantum radar may only query a single polarization, azimuth, elevation, range, Doppler bin at a time. This is an area of development with very promising steps forward[100]. Finally, more advanced technical issues related to random-amplitude targets and radar clutters should also be addressed.

Regarding the experimental challenges for super-

resolution[76], most of the current schemes, from spatial-mode demultiplexing to super-localization by image inversion and heterodyne, rely on the assumption that we need to know the location of the centroid of the sources in order to get full quantum-optimal resolution. In general, this location is not exactly known[76,78–80], so that achieving maximum alignment before estimating the separation becomes an important step in order to optimize the performance in a realistic implementation.

Acknowledgments

1. Nielsen, M. A. & Chuang, I. L. *Quantum Computation and Quantum Information* (Cambridge University Press, Cambridge, 2000).

2. Hayashi, M. *Quantum Information Theory: Mathematical Foundation* (Springer-Verlag, Berlin, 2017).

3. U. L. Andersen, U. L., Neergaard-Nielsen, J. S., van Loock, P. & Furusawa, A. Hybrid discrete- and continuous-variable quantum information. *Nature Phys.* **11**, 713-719 (2015).

4. Serafini, A. *Quantum Continuous Variables: A Primer of Theoretical Methods* (Taylor & Francis, Oxford, 2017).

5. Weedbrook, C. et al. Gaussian quantum information. *Rev. Mod. Phys.* **84**, 621 (2012).

6. Braunstein, S. L. & Van Loock, P. Quantum information with continuous variables. *Rev. Mod. Phys.* **77**, 513 (2005).

7. Adesso, G., Ragy, S. & Lee, A. R. Continuous variable quantum information: Gaussian states and beyond. *Open Systems and Information Dynamics* **21**, 1440001 (2014).

8. Degen, C. L., Reinhard, F. & Cappellaro, P. Quantum sensing. *Rev. Mod. Phys.* **89**, 035002 (2017).

9. Braunstein, S. L. & Caves, C. M. Statistical distance and the geometry of quantum states. *Phys. Rev. Lett.* **72**, 3439 (1994).

10. Braunstein, S. L., Caves, C. M. & Milburn, G. J. Generalized Uncertainty Relations: Theory, Examples, and Lorentz Invariance. *Ann. Phys.* **247**, 135-173 (1996).

11. Giovannetti, V., Lloyd, S. & Maccone, L. Quantum-enhanced measurements: beating the standard quantum limit. *Science* **306**, 1330-1336 (2004).

12. Giovannetti, V., Lloyd, S. & Maccone, L. Quantum metrology. *Phys. Rev. Lett.* **96**, 010401 (2006).

13. Paris, M. G. A. Quantum estimation for quantum technology. *Int. J. Quant. Inf.* **7**, 125-137 (2009).

14. Giovannetti, V., Lloyd S. & Maccone, L. Advances in quantum metrology. *Nature Photon.* **5**, 222 (2011).

15. Braun, D. et al. Quantum enhanced measurements without entanglement. Preprint at https://arxiv.org/abs/1701.05152 (2018).

16. Helstrom, C. W. *Quantum Detection and Estimation Theory* (Academic, New York, 1976).

17. Chefles, A. Quantum state discrimination. *Contemp. Phys.* **41**, 401 (2000).

18. Barnett, S. M. & Croke, S. Quantum state discrimination. *Adv. Opt. Photonics* **1**, 238-278 (2009).

19. Bergou, J. A. , Herzog, U. & Hillery, M. *Discrimination of Quantum States*, in Quantum state estimation, Lecture Notes in Physics, **649**, 417-465 (Springer, Berlin, Heidelberg, 2004).

20. Audenaert, K. M. R. et al. Discriminating States: The Quantum Chernoff Bound. *Phys. Rev. Lett.* **98**, 160501 (2007).

21. Calsamiglia, J., Munoz-Tapia, R., Masanes, L., Acin, A. & Bagan, E., Quantum Chernoff bound as a measure of distinguishability between density matrices: Application to qubit and Gaussian states. *Phys. Rev. A* **77**, 032311 (2008).

22. Pirandola, S. & Lloyd, S. Computable bounds for the discrimination of Gaussian states. *Phys. Rev. A* **78**, 012331 (2008).

23. K. M. R. Audenaert, M. Nussbaum, A. Szkola, and F. Verstraete, Commun. Math. Phys. **279**, 251 (2008).

24. Invernizzi, C., Paris, M. G. A. & Pirandola, S. Optimal detection of losses by thermal probes. *Phys. Rev. A* **84**, 022334 (2011).

25. Spedalieri, G. & Braunstein, S. L. Asymmetric quantum hypothesis testing with Gaussian states. *Phys. Rev. A* **90**, 052307 (2014).

26. Laurenza, R., Lupo, C., Spedalieri, G., Braunstein, S. L. & Pirandola, S. Channel Simulation in Quantum Metrology. Preprint at https://arxiv.org/abs/1712.06603 (2017).

27. Pirandola, S. & Lupo, C. Ultimate precision of adaptive noise estimation. *Phys. Rev. Lett.* **118**, 100502 (2017).

28. Nielsen, M. A. & Chuang, I. L. Programmable Quantum Gate Arrays. *Phys. Rev. Lett.* **79**, 321 (1997).

29. Ji, Z., Wang, G., Duan, R., Feng, Y. & Ying, M. Parameter Estimation of Quantum Channels. *IEEE Trans. Inform. Theory* **54**, 5172–5185 (2008).

30. Kolodynski, J. & Demkowicz-Dobrzański, R. Efficient tools for quantum metrology with uncorrelated noise. *New J. Phys.* **15**, 073043 (2013).

31. Demkowicz-Dobrzański, R. & Maccone, L. Using Entanglement Against Noise in Quantum Metrology. *Phys. Rev. Lett.* **113**, 250801 (2014).

32. Harrow, A. W., Hassidim, A., Leung, D. W. & Watrous, J. Adaptive versus nonadaptive strategies for quantum channel discrimination. *Phys. Rev. A* **81**, 032339 (2010).

33. Pirandola, S., Laurenza, R., Ottaviani, C. & Banchi, L. Fundamental limits of repeaterless quantum communications. *Nat. Commun.* **8**, 15043 (2017). See also Preprint

at https://arxiv.org/abs/1510.08863 (2015).

34. Pirandola, S., Braunstein, S. L., Laurenza, R., Ottaviani, C., Cope, T. P. W., Spedalieri, G. & Banchi, L. Theory of channel simulation and bounds for private communication. Preprint at https://arxiv.org/abs/1711.09909 (2017).

35. Pirandola, S., Quantum Reading of a Classical Digital Memory. *Phys. Rev. Lett.* **106**, 090504 (2011).

36. Lupo, C., Pirandola, S., Giovannetti, V. & Mancini, S. Quantum reading capacity under thermal and correlated noise. *Phys. Rev. A* **87**, 062310 (2013).

37. Spedalieri, G., Lupo, C., Mancini, S., Braunstein, S. L. & Pirandola, S. Quantum reading under a local energy constraint. *Phys. Rev. A* **86**, 012315 (2012).

38. Spedalieri, G. Cryptographic aspects of quantum reading. *Entropy* **17**, 2218-2227 (2015).

39. Pirandola, S., Lupo, C., Giovannetti, V., Mancini, S. & Braunstein, S. L. Quantum Reading Capacity. *New J. Phys.* **13**, 113012 (2011).

40. Lupo, C. & Pirandola, S. Super-additivity and entanglement assistance in quantum reading. *Quantum Inf. Comput.* **17**, 0611 (2017).

41. Guha, S. & Shapiro, J. H. Reading boundless error-free bits using a single photon. *Phys. Rev. A* **87**, 062306 (2013).

42. Guha, S., Dutton, Z., Nair, R., Shapiro, J. H. & Yen, B. Information Capacity of Quantum Reading in Laser Science, OSA Technical Digest,Optical Society of America) paper LTuF2 (2011).

43. Nair, R. Discriminating quantum-optical beam-splitter channels with number-diagonal signal states: Applications to quantum reading and target detection. *Phys. Rev. A* **84**, 032312 (2011).

44. Nair, R. & Yen, B. J. Optimal Quantum States for Image Sensing in Loss. *Phis. Rev. Lett.* **107**, 193602 (2011)

45. Hirota, O., Error Free Quantum Reading by Quasi Bell State of Entangled Coherent States. *Quantum Measurements and Quantum Metrology* **4**, 70-73 (2017).

46. Prabhu Tej, J., Usha Devi, A. R. & Rajagopal A. K. Quantum reading of digital memory with non-Gaussian entangled light. *Phys. Rev. A* **87**, 052308 (2013).

47. Bisio, A., Dall'Arno, M. & D'Ariano, G. M. Tradeoff between energy and error in the discrimination of quantum-optical devices. *Phys. Rev. A* **84**, 012310 (2011).

48. Dall'Arno, M., Bisio, A., D'Ariano, G. M., Miková, M., Ježek, M. & Dušek, M. Experimental implementation of unambiguous quantum reading. *Phys. Rev. A* **85**, 012308 (2012).

49. Dall'Arno, M., Bisio, A., D'Ariano, G.M. Ideal quantum reading of optical memories. *Int. J. Quant. Inf.* **10**, 1241010 (2012).

50. Lloyd, S. Enhanced sensitivity of photodetection via quantum illumination. *Science* **321**, 1463 (2008).

51. Tan, S.-H. et al. Quantum illumination with Gaussian States. *Phys. Rev. Lett.* **101**, 253601 (2008).

52. Shapiro, J. H. & Lloyd, S. Quantum illumination versus coherent-state target detection. *New J. Phys.* **11**, 063045 (2009).

53. Zhuang, Q., Zhang, Z. & Shapiro, J. H. Optimum Mixed-State Discrimination for Noisy Entanglement-Enhanced Sensing. *Phys. Rev. Lett.* **118**, 040801 (2017).

54. Zhuang, Z., Zhang, Z. & Shapiro, J. H. Entanglement-enhanced Neyman–Pearson target detection using quantum illumination. *J. Opt. Soc. Am. B* **34**, 1567 (2017).

55. Barzanjeh, Sh. et al. Microwave quantum illumination. *Phys. Rev. Lett.* **114**, 080503 (2015).

56. Guha, S. & Erkmen, B. I. Gaussian-state quantum-illumination receivers for target detection. *Phys. Rev. A* **80**, 052310 (2009).

57. Xiong, B., Li, X., Wang, X-.Y. & Zhou, L. Improve microwave quantum illumination via optical parametric amplifier. *Ann. Phys.* **385**, 757-768 (2017).

58. Sanz, M., Las Heras, U., García-Ripoll, J. J., Solano, E. & Di Candia, R. Quantum estimation methods for quantum illumination. *Phys. Rev. Lett.* **118**, 070803 (2017).

59. Weedbrook, C., Pirandola, S., Thompson, J., Vedral, V. & Gu, M. How discord underlies the noise resilience of quantum illumination. *New J. Phys.* **18**, 043027 (2016).

60. Ragy, S. et al., Quantifying the source of enhancement in experimental continuous variable quantum illumination, *J. Opt. Soc. Am. B* **31**, 2045–2050 (2014).

61. Wilde, M. M., Tomamichel, M., Lloyd, S., & Berta, M. Gaussian Hypothesis Testing and Quantum Illumination. *Phys. Rev. Lett.* **119**, 120501 (2017).

62. De Palma, G. & Borregaard, J. The ultimate precision of quantum illumination. arXiv:1802.02158 (2018).

63. Lopaeva et al. Experimental realization of quantum illumination. *Phys. Rev. Lett.* **110**, 153603 (2013).

64. Meda, A., Losero, E., Samantaray, N., Scafirimuto, F., Pradyumna, S., Avella, A., Ruo-Berchera, I. & Genovese, M. Photon-number correlation for quantum enhanced imaging and sensing. *J. Opt.* **19**, 094002 (2017).

65. Zhang, Z., Tengner, M., Zhong, T., Wong, F. N. C. & Shapiro, J. H. Entanglement's benefit survives an entanglement-breaking channel. *Phys. Rev. Lett.* **111**, 010501 (2013).

66. Zhang, Z., Mouradian, S., Wong, F. N. C. & Shapiro, J. H. Entanglement-enhanced sensing in a lossy and noisy environment. *Phys. Rev. Lett.* **114**, 110506 (2015).

67. Las Heras, U., Di Candia, R., Fedorov, K. G., Deppe, F., Sanz, M. & Solano, E. Quantum illumination reveals phase-shift inducing cloaking. *Sci. Rep.* **7**, 9333 (2017).

68. M. Lanzagorta, *Quantum Radar (Synthesis Lectures on Quantum Computing)*, Vol. 3, No. 1, pp. 1-139 (Morgan & Claypool, 2011).

69. Tsang, M., Nair, R. & Lu, X.-M. Quantum theory of superresolution for two incoherent optical point sources. *Phys. Rev. X* **6**, 031033 (2016).

70. Lupo, C. & Pirandola, S. Ultimate precision bound of quantum and subwavelength imaging. *Phys. Rev. Lett.* **117**, 190802 (2016).

71. Nair, R. & Tsang, M. Far-Field Superresolution of thermal electromagnetic sources at the quantum limit. *Phys. Rev. Lett.* **117**, 190801 (2016).

72. Kerviche, R., Guha, S. & Ashok, A. Fundamental limit of resolving two point sources limited by an arbitrary point spread function. Preprint at https://arxiv.org/abs/1701.04913 (2017).

73. Rehacek, J., Paúr, M., Stoklasa, B., Hradil, Z. & Sánchez-Soto, L. L. Optimal measurements for resolution beyond the Rayleigh limit. *Opt. Letters* **42**, 231-234 (2017).

74. Yang, F., Nair, R., Tsang, M., Simon, C. & Lvovsky, A. I. Fisher information for far-field linear optical superresolution via homodyne or heterodyne detection in a higher-order local oscillator mode. *Phys. Rev. A* **96**, 063829 (2017).

75. Lu, X.-M., Krovi, H., Nair, R., Guha, S., Shapiro, J. H. Quantum-optimal detection of one-versus-two

incoherent optical sources with arbitrary separation, arXiv:1802.02300 (2018).

[76] Tang, Z. S., Durak, K. & Ling, A. Fault-tolerant and finite-error localization for point emitters within the diffraction limit. *Opt. Express* **24**, 22004 (2016).

[77] Nair, R. & Tsang, M. Interferometric superlocalization of two incoherent optical point sources. *Opt. Express* **24**, 3684-3701 (2016).

[78] Yang, F., Taschilina, A., Moiseev, E. S., Simon, C. & Lvovsky, A. I. Far-field linear optical superresolution via heterodyne detection in a higher-order local oscillator mode. *Optica* **3**, 1148 (2016).

[79] Tham, W. K., Ferretti, H. & Steinberg, A. M. Beating Rayleigh's Curse by Imaging Using Phase Information. *Phys. Rev. Lett.* **118**, 070801 (2017).

[80] Paúr, M., Stoklasa, B., Hradil, Z., Sanchez-Soto, L. L. & Řeháček, J. Achieving the ultimate optical resolution. *Optica* **3**, 1144-1147 (2016).

[81] Gatto Monticone, D. et al. Beating the Abbe Diffraction Limit in Confocal Microscopy via Nonclassical Photon Statistics. *Phys. Rev. Lett.* **113**, 143602 (2014).

[82] Treps, N., Andersen, U. L., Buchler, B., Lam, P. K., Maître, A., Bachor, H.-A. & Fabre, C. Surpassing the Standard Quantum Limit for Optical Imaging Using Nonclassical Multimode Light. *Phys. Rev. Lett.* **88**, 203601 (2014).

[83] Classen, A. et al. Superresolving imaging of arbitrary one-dimensional arrays of thermal light sources using multiphoton interference. *Phys. Rev. Lett.* **117**, 253601 (2016).

[84] Tsang, M. Quantum imaging beyond the diffraction limit by optical centroid measurements. *Phys. Rev. Lett.* **102**, 253601 (2009).

[85] Rozema, L. A. et al. Scalable spatial superresolution using entangled photons. *Phys. Rev. Lett.* **112**, 223602 (2014).

[86] Chiribella, G., D'Ariano, G. M. & Perinotti, P. Quantum circuit architecture. *Phys. Rev. Lett.* **101**, 060401 (2008).

[87] Bennett, C. H. et al. Teleporting an unknown quantum state via dual classical and Einstein-Podolsky-Rosen channels. *Phys. Rev. Lett.* **70**, 1895 (1993).

[88] Braunstein, S. L. & Kimble, H. J. Teleportation of continuous quantum variables. *Phys. Rev. Lett.* **80**, 869-872 (1998).

[89] Pirandola, S., Eisert, J., Weedbrook, C., Furusawa, A & Braunstein, S. L. Advances in quantum teleportation. *Nat. Photonics* **9**, 641-652 (2015).

[90] Monras, A. & Paris, M. G. A. Optimal quantum estimation of loss in bosonic channels. *Phys. Rev. Lett.* **98**, 160401 (2007).

[91] Banchi, L., Braunstein, S. L. & Pirandola S. Quantum fidelity for arbitrary Gaussian states. *Phys. Rev. Lett.* **115**, 260501 (2015).

[92] Adesso, G., Dell'Anno, F., Siena, S. D., Illuminati, F. & Souza, L. A. M. Optimal estimation of losses at the ultimate quantum limit with non-Gaussian states. *Phys. Rev. A* **79**, 040305(R) (2009).

[93] Fuchs, C. A. & van de Graaf, J. Cryptographic distinguishability measures for quantum-mechanical states. *IEEE Trans. Inf. Theory* **45**, 1216 (1999).

[94] Sudarshan, E. C. G. Equivalence of Semiclassical and Quantum Mechanical Descriptions of Statistical Light Beams. *Phys. Rev. Lett.* **10**, 277 (1963).

[95] Glauber, R. J. Coherent and Incoherent States of the Radiation Field. *Phys. Rev.* **131**, 2766 (1963).

[96] Modi, K., Brodutch, A., Cable, H., Paterek, T. & Vedral, V. The classical-quantum boundary for correlations: Discord and related measures. *Rev. Mod. Phys.* **84**, 1655 (2012).

[97] Barzanjeh, Sh., Vitali, D., Tombesi, P. & Milburn, G. J. Entangling optical and microwave cavity modes by means of a nanomechanical resonator. *Phys. Rev. A* **84**, 042342 (2011).

[98] Barzanjeh, Sh., Abdi, M., Milburn, G. J., Tombesi, P. & Vitali. Reversible Optical-to-Microwave Quantum Interface. D. *Phys. Rev. Lett.* **109**, 130503 (2012).

[99] Andrews, R. W. et al. Bidirectional and efficient conversion between microwave and optical light. *Nat. Phys.* **10**, 321 (2014).

[100] Zhuang, Q., Zhang, Z. & Shapiro, J. H. Entanglement-enhanced lidars for simultaneous range and velocity measurements. *Phys. Rev. A* **96**, 040304(R) (2017).